Supporting Information

Sensor-integrated Gut-on-a-Chip for Monitoring Senescence-Mediated Changes in the Intestinal Barrier

Konstanze Brandauer[a], Alexandra Lorenz[a], Silvia Schobesberger[a], Patrick Schuller[a], Martin Frauenlob[a], Sarah Spitz[a,b], and Peter Ertl[a,b,*]

Table of content:

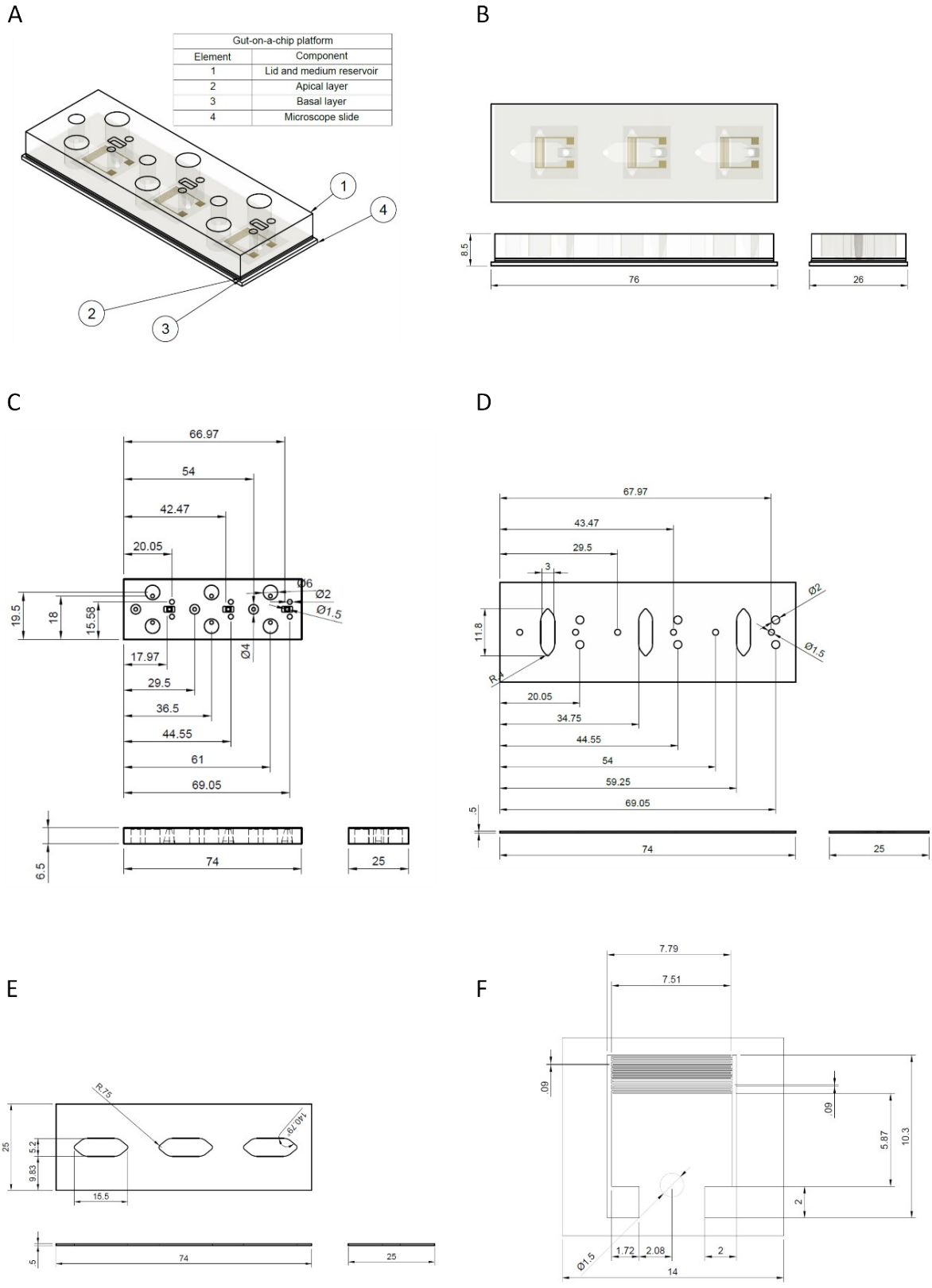

***Figure SI 1**: (A) Render of the gut-on-the chip platform. (B) Technical drawing of the entire microfluidic system. (C) Technical drawing of the cast PDMS lid with medium reservoirs. (D) Technical drawing of the apical layer. (E) Technical drawing of basal layer and (F) technical drawing of the electrode. All dimensions are in millimeters (mm).*

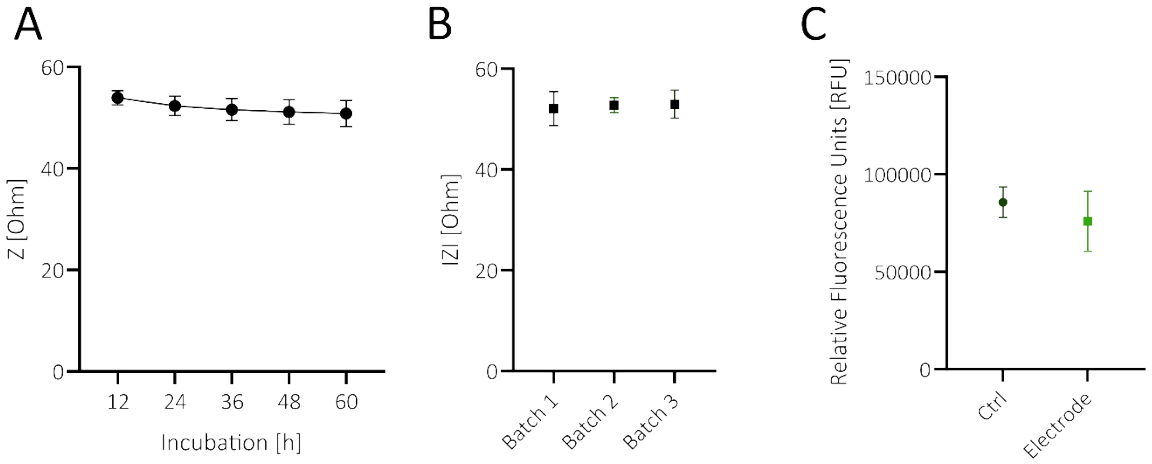

***Figure SI 2**: (A) Continuous impedance measurements at 20 kHz (right, n=3, P=0.4539, ns not shown) revealing no significant impedance changes over time. (B) Impedance measurements of three different electrode batches, each coated with 1% collagen and tested in full medium at 20kHz, showed no significant differences between the batches (n=3, data displayed as mean +/- SD, P=0.8292, ns not shown). Statistical significance was determined by an Ordinary one-way ANOVA. (B) Relative Fluorescence Units of the PrestoBlue™ Assay, revealing no significant difference between cells grown on a bare membrane*

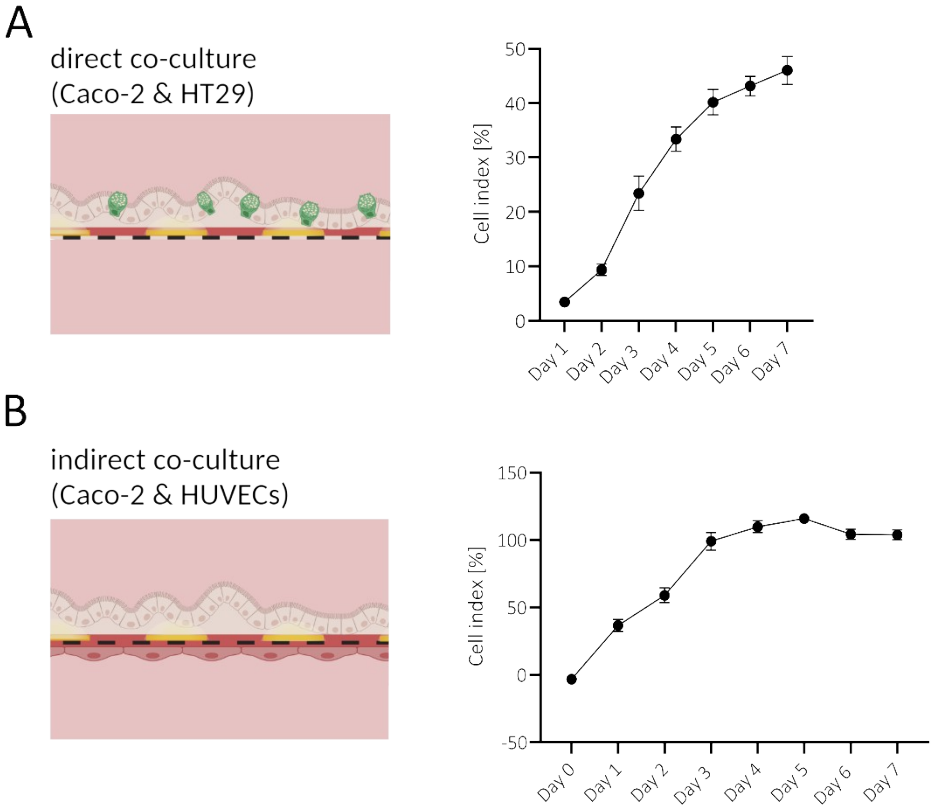

***Figure SI 3:** (A) Cell index (CI) of the direct co-culture exponentially increases over time, reaching a plateau at ~45% on day 7. (B) In contrast, the indirect co-culture with epi- and endothelial cells shows a more rapid increase in CI, plateauing at ~110% after just 4 days, indicative of the establishment of two distinct barriers.*

and electrodes after 48h (n=9, data displayed as mean +/- SD, P=0.1091, ns not shown). Statistical significance was determined by an unpaired t-test.

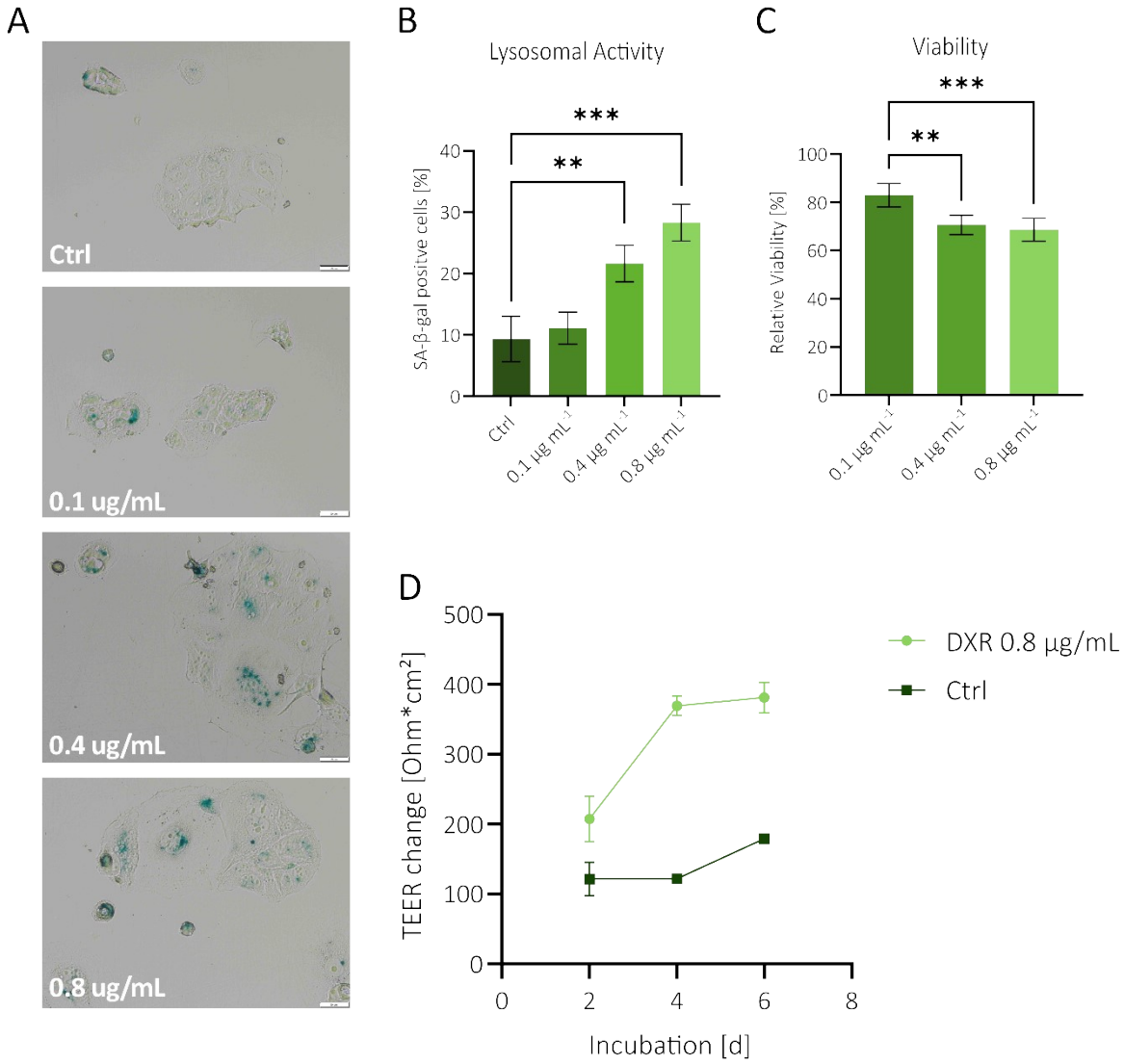

***Figure SI 4**: (A) Brightfield images following the SA-ß-galactosidase assay taken with 20x magnification. Senescent-positive cells are stained blue. Scale bars are 50 µm. (B) Percentage of SA-ß-gal-positive cells after the addition of increasing concentrations of DXR for 5 days. Statistical analysis was performed using an ordinary one-way ANOVA and Dunnett's multiple comparisons test (n=3; **P= 0.0033, ***P=0.0002, ns are not shown). (C) Impact of different DXR concentrations on the cellular viability after a 2-day exposure (n=3; **P= 0,0017, ***P= 0.0007, ns are not shown). (D) TEER change after the exposure of 0.8 µg/mL DXR (n=3).*

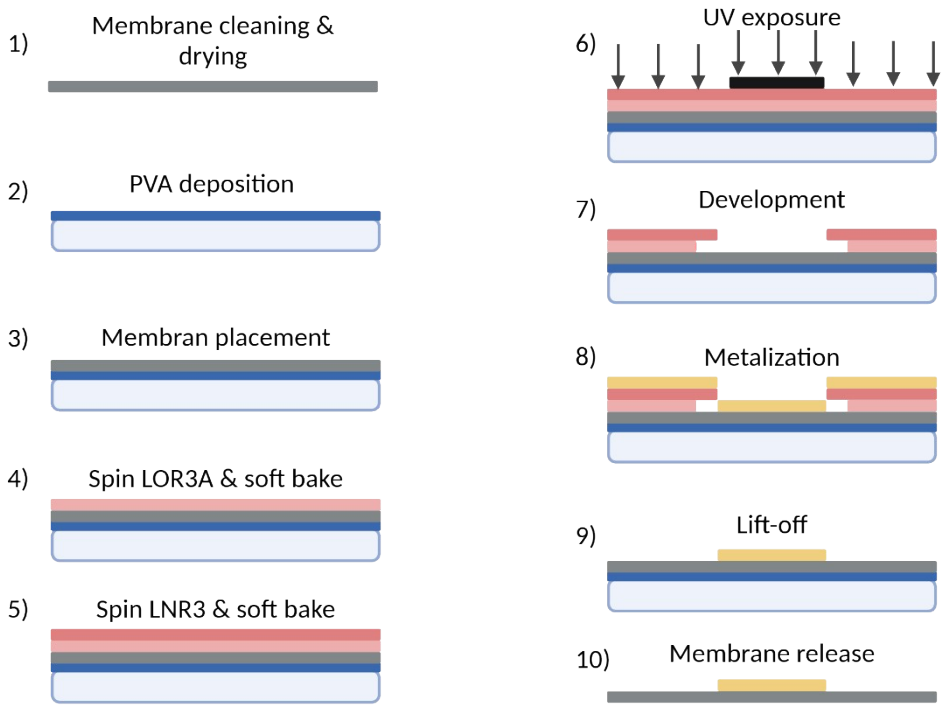

Figure SI 5: *Illustration of the gold electrode fabrication*

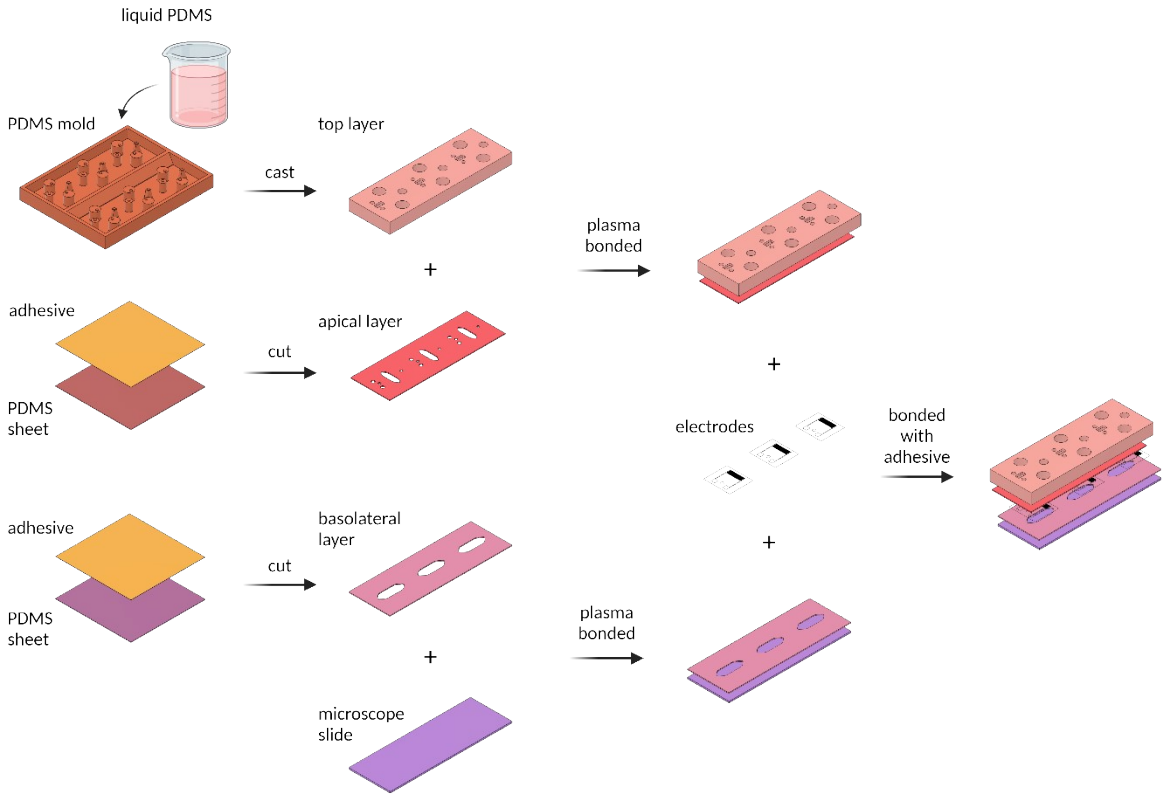

Figure SI 6*: Illustration of the chip fabrication*

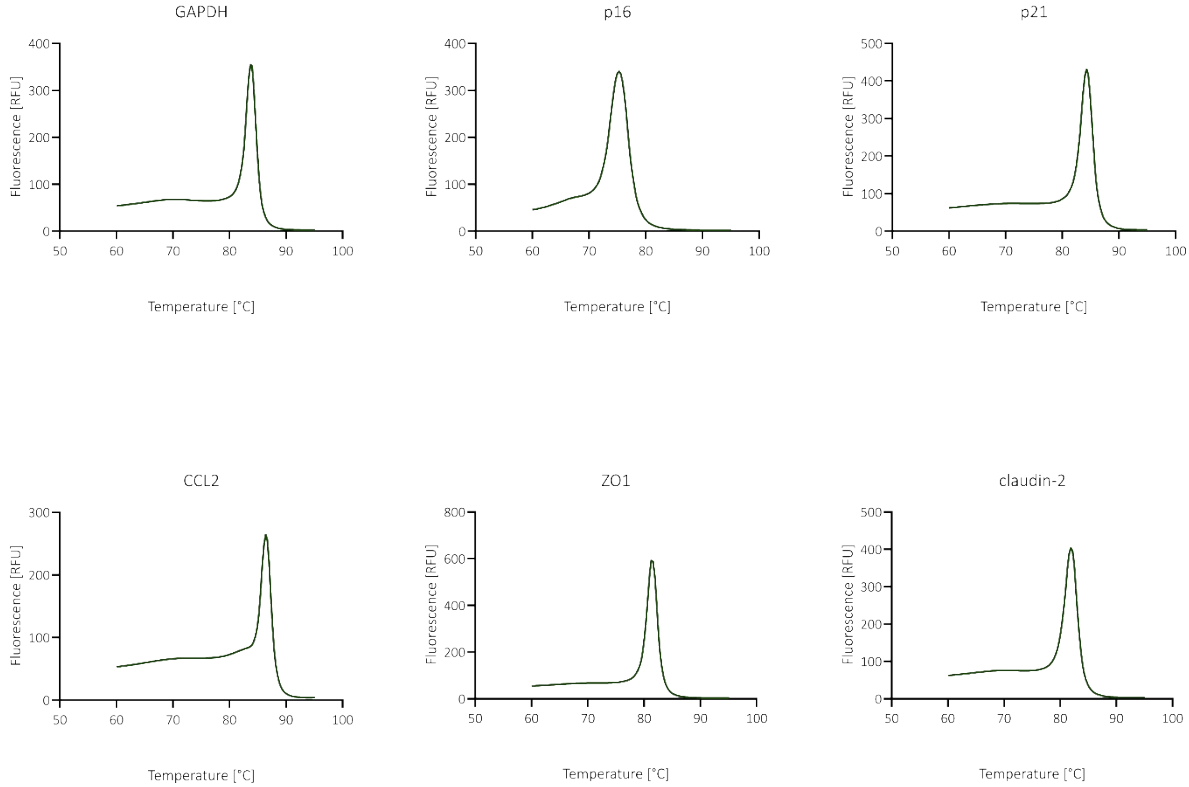

Figure SI 7: *Melting curves of the applied primers reveal single peaks, indicating that amplicons of one particular length are synthesized.*

Table SI 1*: Genes and their primer sequences used for qPCR*

Gene	Function	Primer sequence
GAPDH	Oxidoreductase in glycolysis and gluconeogenesis	Fw: TGGGTGTGAACCATGAGAAGT Rv: TGAGTCCTTCCACGATACCAA
p16	Cyclin-dependent kinase inhibitor 2A	Fw: TTCCCCCACTACCGTAAATGT Rv: GCTCACTCCAGAAAACTCCAAC
p21	cyclin-dependent kinase inhibitor 1A	Fw: AGGTGGACCTGGAGACTCTCAG Rv: TCCTCTTGGAGAAGATCAGCCG
CCL2	C-C motif chemokine 2	Fw: AGACTAACCCAGAAACATCC Rv: ATTGATTGCATCTGGCTG
ZO1	Tight-junction adapter protein	Fw: CGCACAGTTTGGCACAGC Rv: GCCACCACAGTATGACCATCTT
Claudin-2	Pore-forming protein	Fw: TGGATCGTGTCAGAAGGTGC Rv: ACACTAGCCCCCATTTCTGC